The Design Evolution of a Sensing and Force-Feedback Exoskeleton Robotic Glove for Hand Rehabilitation Application

Pinhas Ben-Tzvi
Robotics and Mechatronics Laboratory,
Mechanical Engineering Department,
Virginia Tech,
635 Prices Fork Road (0238),
Blacksburg, VA 24061
e-mail: bentzvi@vt.edu

Jerome Danoff
Milken Institute School of Public Health,
Department of Exercise and Nutrition Sciences,
The George Washington University,
950 New Hampshire Avenue, NW,
Washington, DC 20052

Zhou Ma
US Med Innovations,
6930 Carroll Avenue,
Takoma Park, MD 20912

This paper presents the design evolution of the sensing and force-feedback exoskeleton robotic (SAFER) glove with application to hand rehabilitation. The hand grasping rehabilitation system is designed to gather kinematic and force information from the human hand and then playback the motion to assist a user in common hand grasping movements, such as grasping a bottle of water. Grasping experiments were conducted where fingertip contact forces were measured by the SAFER glove. These forces were then modeled based on a machine learning approach to obtain the learned contact force distributions. Using these distributions, fingertip force trajectories were generated with a Gaussian mixture regression (GMR) method. To demonstrate the glove's effectiveness to manipulate the hand, experiments were performed using the glove to demonstrate grasping capabilities on several objects. Instead of defining a grasping force, contact force trajectories were used to control the SAFER glove in order to actuate a user's hand while carrying out a learned grasping task. [DOI: 10.1115/1.4032270]

1 Introduction

Significant work has been presented in the field of haptic gloves, particularly in the application of rehabilitation [1,2]. However, many challenges persist within this field in comparison to well-developed force-feedback rehabilitation devices for larger body areas such as upper [3,4] and lower limbs [5,6] due to the hand's smaller size and rich sensing and motion capabilities [7].

Haptic gloves (that are capable of generating force) for rehabilitation are still in an early stage of development and they have yet to be commonly used in clinical applications [1]. The two major types of haptic gloves could be categorized based on their means of attachment as: (1) body-based/portable haptic gloves [8–15] and (2) ground-based haptic gloves [16–21].

In the case of portable haptic gloves, they fit over the user's hand and are capable of a wide range of motion in comparison to the ground-based devices. In addition, they can measure and actuate the fingers' motion more easily since they are more kinematically similar to human hands. However, the glove's excessive weight becomes an issue due to fatigue caused by prolonged use that can cause pain in the user's limbs. Unlike portable haptic gloves, ground-based devices are fixed and designed to be used while the user is sitting. Thus, the user's range of motion is limited when compared to portable haptic gloves. Other work in hand rehabilitation devices also includes soft gloves with cable and fluidic actuators [22–24].

The design of a self-contained body-based robotic haptic exoskeleton glove (SAFER) was previously demonstrated to measure the user's hand motion and assist hand motion while remaining portable and lightweight [25–27]. The exoskeleton glove comprises an articulated five-finger mechanism with each finger actuated with miniature DC motors using antagonistically routed cables at the finger, which act as both active and passive force actuators. The five-finger mechanism mounts over the dorsum of a bare hand and is easily adapted to fit to a wide variety of finger sizes without constraining the fingers' range of motion while providing haptic force feedback to each finger. The glove system is able to accurately and comfortably track the complex motion of the fingers related to common movements of hand functions.

The main contribution of this paper over Ref. [27] is the detailed consideration of the system's design evolution and the mechanism/hardware design aspects, which is supplemented by an application of the latest design generation for a hand rehabilitation learning system. The hand rehabilitation learning system is capable of learning patterns from recorded fingertip motion and contact force data so that the glove can then assist the user to grasp different objects. The paper is organized as follows: Section 2 introduces the SAFER glove system and its design evolution. Section 3 provides an overview of the rehabilitation learning system. Section 4 discusses how each module of the system is implemented with the glove system. Section 5 describes preliminarily experiments to evaluate the proposed system. Section 6 provides the conclusions and future work.

2 Glove Mechanism System Design

2.1 Mechanical Design. The five-fingered haptic glove is a portable sensing/actuating system that fits on a bare hand and is attached to the finger tips as shown in Fig. 1. In order to lighten and simplify the device, the movements of the metacarpophalangeal, proximal interphalangeal, and distal interphalangeal joints of each finger are coupled together with one actuator module. The actuator unit consists of a brushed DC motor. The speed of the finger motion can be adjusted for the needed application. Cable transmission is chosen because it can provide adequate power through narrow pathways and allow the actuator to be located away from the dexterous fingers. Therefore, two Dyneema® cables are attached to the pulley and routed along the exoskeleton to the fingertip. Bidirectional force control is enabled by antagonistically actuating the two cables, thereby transferring this force along the exoskeleton to the fingertip.

The components of the five-fingered glove form a series of three linkages over each individual finger. For safety, the mechanism limits the range of motion of the fingers and the thumb. Due to the unusual geometry of the thumb joint and its large workspace, the three linkage design is not possible to comfortably and repeatedly secure an exoskeleton mechanism to the thumb's

Manuscript received September 12, 2015; final manuscript received December 9, 2015; published online May 4, 2016. Assoc. Editor: Venkat Krovi.

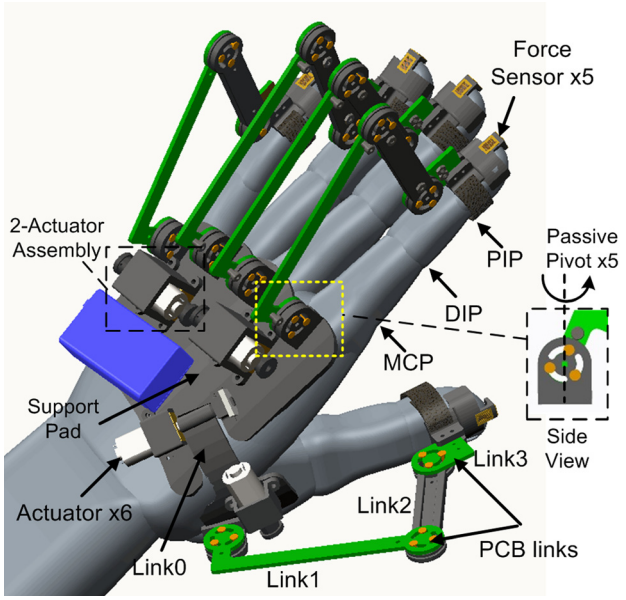

Fig. 1 CAD model of the hand and SAFER glove system

proximal link. Thus, one more link was added to the thumb base to decouple off-axis movements. More information on the design details is available in Ref. [26].

2.2 Kinematics of the Compound Hand-Mechanism System. Figure 2(*a*) illustrates the side view of a hand with the SAFER glove mechanism in a bent configuration. For each finger, the haptic mechanism and the finger itself can be modeled as a single six-bar mechanism, as shown in Fig. 2(*b*), where the hand/support pad represents the ground link. Each finger consists of three links, and the haptic mechanism for each finger consists of three links as well. However, the terminal link of each finger is rigidly connected to the terminal link of the haptic mechanism. Therefore, there are six links in total (including one ground link) and six revolute pin connections. Based on Fig. 2(*b*), the fingertip position can be found in terms of the mechanism joint angles (α_1, α_2, and α_3). If the mechanism joint angles α_i are measured and finger lengths l_i are known, the exact finger position can be calculated. More details on the kinematics analyses are available in Ref. [26].

2.3 Workspace of the Compound Hand-Mechanism System. The size and shape of human fingers may vary between individuals and among different fingers for each person. To meet universal needs in a cost-effective manner, it is desirable to accommodate a large number of users by using a single and adaptable design. Through study of anthropomorphic data and optimization analysis [26], optimum linkage lengths were selected for each link of the glove mechanism. Because a single actuator drives the three links, this property not only makes the glove simpler and lighter, but it also allows the finger mechanism to be self-adapting to variations in finger sizes.

Figures 3(*a*) and 3(*b*) illustrate that the finger workspace is a subset of the mechanism's workspace for both index and thumb fingers, thereby ensuring the glove allows unimpeded finger motion. This means that the new mechanism design should ideally cover the hand's entire workspace.

2.4 Design Generations of the SAFER Glove. In the past 3 years, three generations of the SAFER glove system were developed based on a similar design concept. Figure 4 shows all three design generations worn on a hand from both front and back

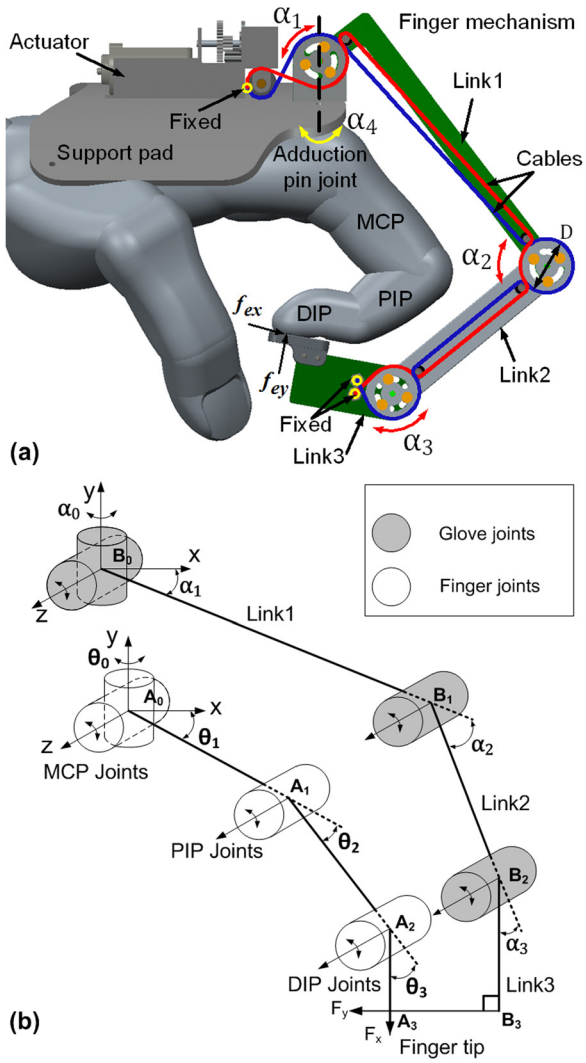

Fig. 2 (*a*) CAD model of the index finger mechanism of the glove showing the cable transmission model and (*b*) kinematic diagram of the finger–glove system

views. The main differences of these design generations are summarized in Table 1.

The worm-gear motor that was used in the first generation provides up to 35 N passive force feedback due to its nonback drivable feature, but the backlash of the worm-gear introduced slow mechanical response [15]. Therefore, the worm-gear motor was replaced by miniature DC motors with high reduction ratio in subsequent design generations.

The printed circuit board (PCB) links in the current design serve not only as the electrical components carrier but also as mechanical links, which greatly reduced the weight of the system, but also reduced the maximum output force due to the limited mechanical strength of the PCB material. Thus, in the third design generation, the links' material was changed to aluminum in order to increase the strength and thereby increasing the allowable active force output from 10 N to 15 N on the account of slightly increasing the weight of the glove system.

In the second design generation, the strain gauge sensor used can accurately measure the contact force, but in order to accommodate the sensor, the fingertip links were made of 3D printed parts, which were difficult to adapt to different finger sizes. Thus, in the third design generation, force sensing resistors (FSR) were used to measure the contact force due to its advantages, which include low cost, small thickness, and flexibility. The drawback with using FSR was that the user could not feel the tactile

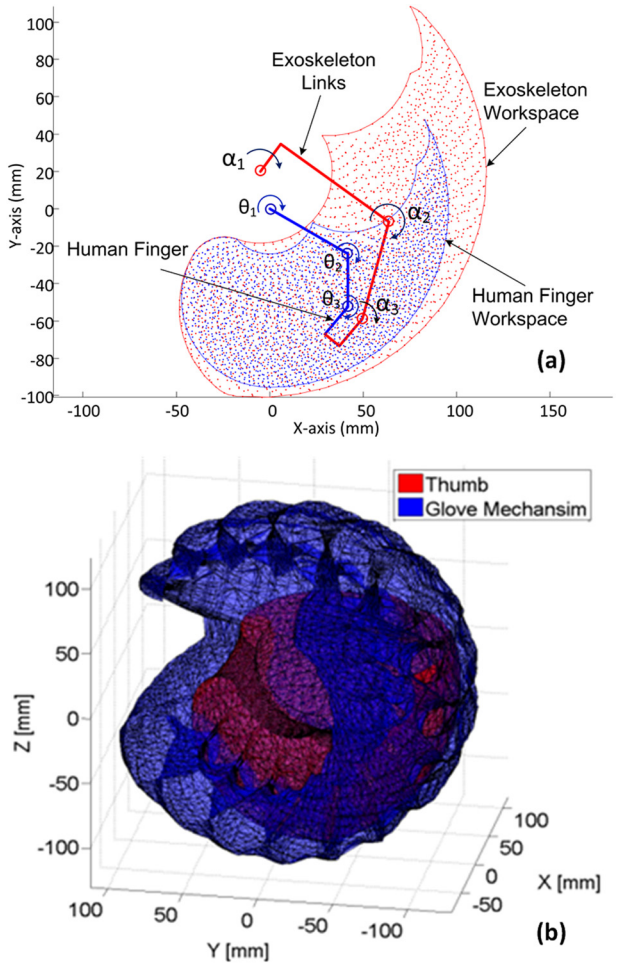

Fig. 3 (*a*) Two-dimensional workspace comparison between index finger and the glove mechanism and (*b*) 3D workspace of the thumb (inner workspace) versus glove thumb mechanism (outer workspace)

information from the object because the sensor was placed between the fingertip and the object. Apart from these variations, the mechanical design of all three generations is almost identical.

3 The Proposed Rehabilitation Learning System

3.1 Rehabilitation System Overview. A preliminary grasping learning and rehabilitation system is proposed that is capable of measuring and learning from human grasping to provide rehabilitation functions to the user. The overview of the system is shown in Fig. 5 consisting of four main components: the demonstration procedure, the SAFER glove system, the machine learning algorithm, and the rehabilitation procedure. The main components of the whole system are the SAFER glove and the learning algorithm. During the grasping procedure demonstration, the SAFER glove measures both motion and contact force information in the grasping procedure demonstration. The captured motion and force data from the procedures are used to train a Gaussian mixture model (GMM) [28], which represents the joint distribution of the data. The learned motion and force information are then mapped to the SAFER glove to actuate a wooden hand (or user) to generate proper motions and force to accomplish the learned tasks. The user can watch and manipulate the virtual hand and objects in a head-mounted device in 3D using the graphical user interface (GUI).

The grasping motion replication process from the collected demonstration data is divided into four stages: (a) record the demonstration procedure for common grip and release patterns; (2) process and align the motion and force sequences from different trials using a dynamic time warping (DTW) method [29]; (3) encode the processed demonstration sequences using GMM (a machine learning approach); and (4) generate the motion and force sequences from the GMM by GMR to produce learning results that are then applied on the glove to reproduce grasping motions.

3.2 Description of the Hand Exoskeleton Mechanism. The articulated finger mechanism provides flexion/extension and abduction/adduction at the proximal joint, and the glove mechanism configuration (Fig. 6) allows the glove mechanism to adapt to different finger sizes. Miniature DC motors with high reduction ratio and an antagonistically routed cable mechanism at each finger are used as both active and passive force display actuators. This design minimizes the size and weight of the mechanism while maximizing its workspace and force output range of the glove. Since all necessary components are lightweight and contained inside the glove, the user can move each finger freely without being tethered or feeling fatigued.

To address the workspace challenge such that the human operator's motion is not restricted by the haptic device, a multilink mechanism was chosen based on this reasoning because it is more suitable for multiple finger inputs and has a larger workspace [25,26]. By analyzing anthropomorphic data and optimization analysis [30], optimum linkage lengths were selected for each link of the glove mechanism. As a result, the new mechanism design can ideally cover most of the finger's workspace. In other words, the glove links allow full flexion and extension in all joints. Furthermore, this mechanism does not have any limit in adduction/abduction direction since movement in these directions will not affect the cable length change. Thus, the SAFER glove can provide adequate degrees-of-freedom and sufficient workspace for the operator's hand.

The whole system weighs 430 g. This includes the glove skeleton and mechanism, battery, actuator unit, control system, and wireless module. Besides being lightweight and a self-contained actuator system, the SAFER glove is also highly portable and capable of wireless operation. Three rotational sensors located on each finger provide accurate joint angle data to calculate the finger position. Force sensors and a shunt circuit for measuring the motor current are also integrated into the mechanism. Thus, for each finger, three joint angles and torque/force measurements are available in a highly compact package for feedback control and for data collection with no need for an additional glove or measurement equipment.

The main advantages of the SAFER glove are listed as follows: (1) the system is lightweight, which reduces user fatigue. Wireless communication capability with a PC or a mobile robot makes the system highly portable; (2) the mechanical design is compact and designed such that it does not limit the natural range of motion of human fingers; (3) the system can accurately measure the hand kinematics and provide force-feedback information; (4) the SAFER glove is low in production cost making it applicable to large-scale production to address the needs of large number of rehabilitation patients; and (5) the system is safe and can run for over 1 hr of continuous operation.

3.3 Learning System for Finger Motion/Force. The learning procedure is used to actuate/assist the patient's hand in order to reproduce similar grasping motions as recorded in the demonstration phase. It should be noted that data are different across demonstration trials due to slightly different initial positions, speed, joint angles, etc. Therefore, the grasp should be modeled from the demonstration data to generalize across multiple stored trials. In this section, a statistical modeling approach is used to train a learning model with the human demonstration data, so that the SAFER glove can learn the high dimensional motion and force pattern from human hand functions.

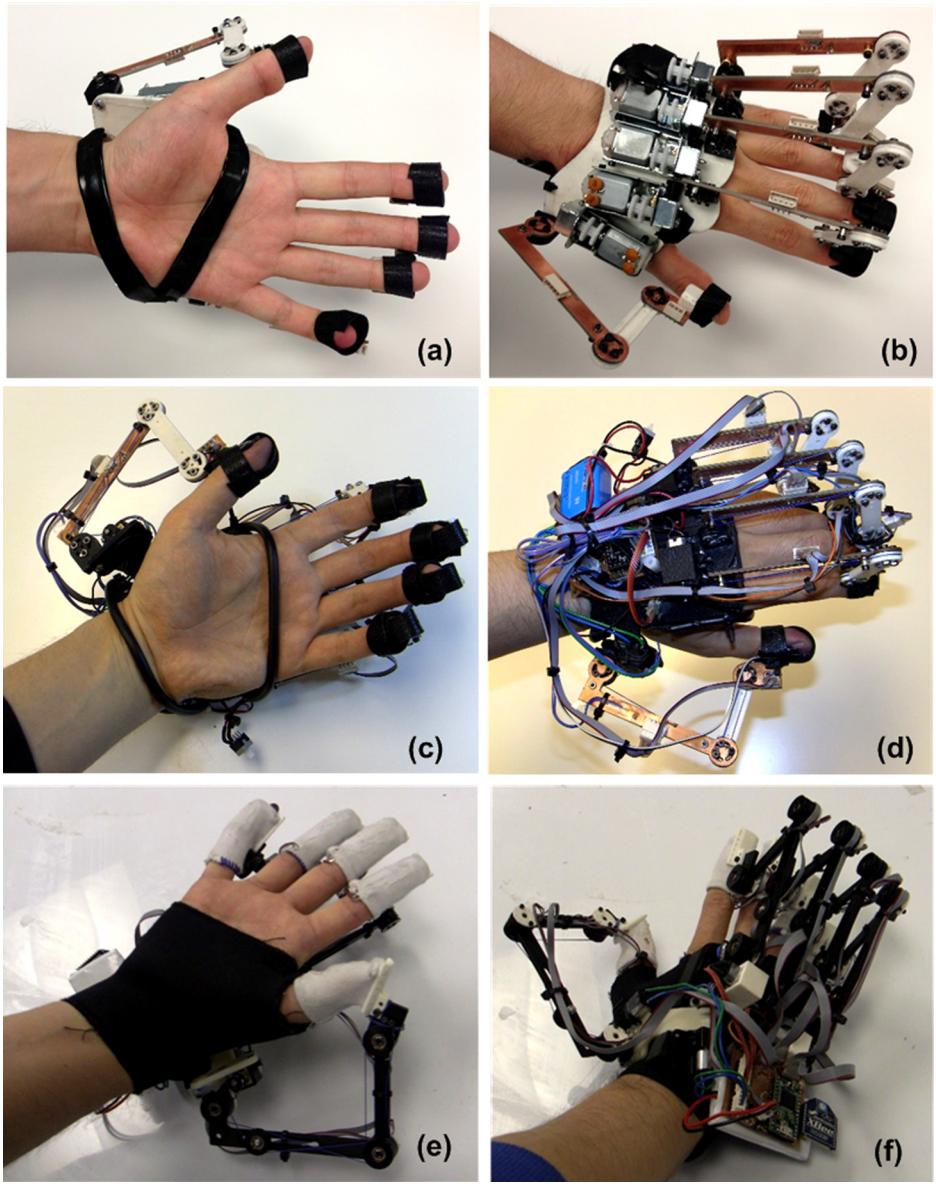

Fig. 4 Three generations of the SAFER glove prototype worn on a hand: (*a*) and (*b*) first generation, (*c*) and (*d*) second generation, and (*e*) and (*f*) third generation

The motion and force data can be treated as a high dimensional time series. The sequences of multiple subjects performing similar activities vary slightly in terms of the magnitude and velocity of the motions. DTW is well known as a temporal alignment technique to find an optimal alignment of multiple time series. Intuitively, the sequences are warped nonlinearly to match each other. DTW has been widely used in the field of machine learning, such as in speech recognition, activity recognition, and synthesis of human motion for animation. A typical DTW method is applied here that uses an optimization approach to find the optimal alignment of the data sequence to a reference sequence. This method minimizes the sum of squares of the vertical distance between the reference sequence and the aligned sequence. Figure 7 shows sample DTW results after aligning motion data [27].

This statistical modeling approach is used to encode human behavior while taking into consideration the variance existing among multiple trials and subjects (for the same behavior). Given a data set $\xi_j = \{\xi_{j,t}, \xi_{j,m}, \xi_{j,f}\}_{j=1}^{N}$ of human demonstration (where N is the number of observations, $\xi_{j,t}$ is the time stamp, $\xi_{j,m} \in \Re^D$ is the D-vector of motion sequence, D is the number of joints, and $\xi_{j,f} \in \Re^3$ is the force vector), the data set can be represented by a probabilistic model, the GMM, which is a mixture of K Gaussian distributions. The mixture component was defined by $K = 3$ because the grasping process was segmented into three major states including: (i) grasp the object, (ii) lift and place back the object, and (iii) release the object.

Table 1 Comparison of the three design generations of the SAFER glove

Actuator type/No.	First generation Worm-gear/5	Second generation DC motor/6	Third generation DC motor/6
Link material	PCB[a] and plastic	PCB and plastic	Metal
Weight	310 g	275 g	410 g
Max. active force	10 N	10 N	15 N
Force sensor	FSR sensor	Strain gauge	FSR sensor

[a]PCB—Printed circuit board.

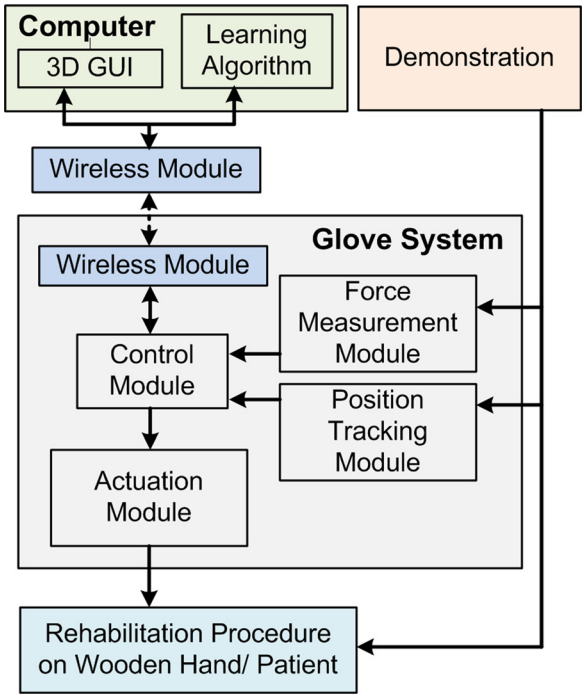

Fig. 5 Overview of the rehabilitation learning system

3.4 Learning Result Mapping to a Passive Hand. For a given joint probability distribution $p(\xi_t, \xi_m)$ and $p(\xi_t, \xi_f)$ of the dataset modeled by the GMM, the GMR computes a generalized trajectory by estimating $E[p(\xi_m|\xi_t)]$ and $E[p(\xi_f|\xi_t)]$, thus retrieving a motion point and a force point at each time step ξ_t.

Subsequently, the glove is controlled to follow these motion and force trajectories by generating the grasping patterns in playback fashion to actuate/assist a wooden (or diseased) hand to accomplish these movements. The glove adapts a hybrid motion and force controller to ensure that the fingers of the user's hand keep contact with the object with a certain force, based on the GMR. In this system, only the normal force is controlled due to the limitation of the FSR sensor used.

3.5 Training Rehabilitation With a 3D GUI. The developed GUI provides both force and motion information of the hand for the user and hand therapist to view, and a virtual–reality environment to interact with the glove system for the purpose of hand rehabilitation exercising.

Haptic gloves are used both to mediate the user's input into the 3D GUI simulation and to provide feedback from the simulation in response to this input. Thus, the haptic glove has both sensory and display channels.

During virtual–reality hand exercising, the haptic glove contact surfaces transmit important sensory information that helps users grasp and manipulate virtual objects in the environment. When added to 3D visual feedback, haptic feedback greatly improves simulation realism [9,31].

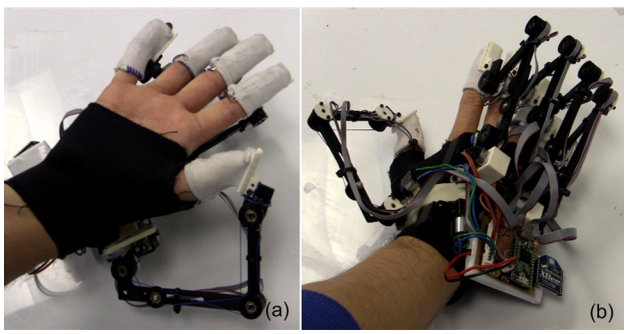

Fig. 6 SAFER glove prototype worn on a right hand

4 Implementation of the System

4.1 Tracking of the Finger Position. Three miniature plastic precision potentiometers with a precision of 0.09 deg (12 bit AD converter) measure three joint positions of each user's finger. Wires from each encoder are routed through the finger links and then connected to the main controller. The length of the connection cables and the connections is optimized to minimize the resistive losses since the sensors produce an analog signal. Sampling of the tracking information is done using an AD multiplexer and a 12-bit AD converter on the main controller at more than 1000 Hz.

The dimensions of each link segment are known a priori and used by the direct kinematics computational model stored in the controller. This model allows the determination of the position and orientation of each fingertip relative to the palm, based on the real-time position readings of the encoder sensors.

The method of using encoders and links to track the finger positions has advantages in comparison to other tracking systems. Our method is simpler and more user friendly. Its accuracy is fairly constant over the whole finger workspace and depends essentially on the resolution of the encoder sensors used. Unlike electromagnetic tracking systems, our method is not influenced by interferences with metallic structures or magnetic fields that may exist in the design. Furthermore, the encoder tracking method has very low jitter and the lowest latency of all tracking types.

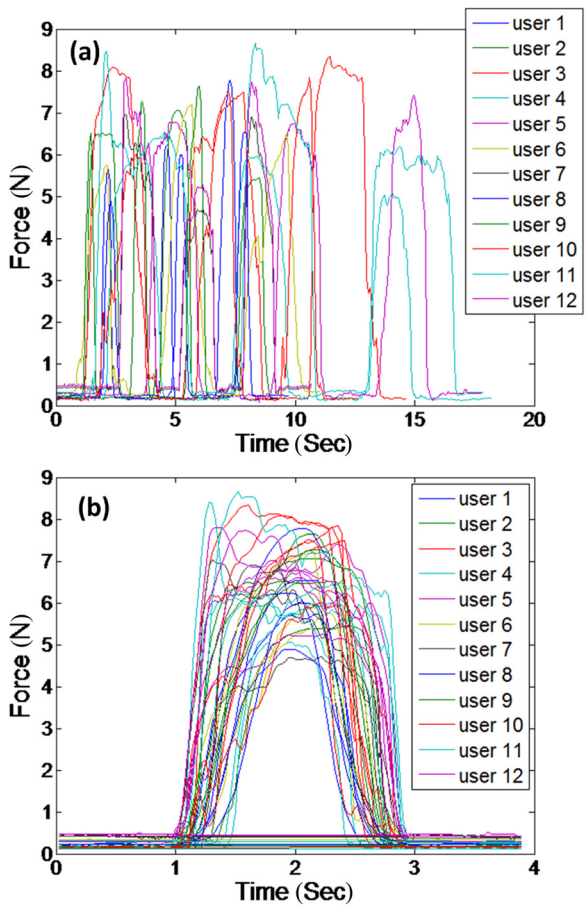

Fig. 7 DTW result for index force data related to grasping a bottle of water experiment: (*a*) raw data and (*b*) DTW results

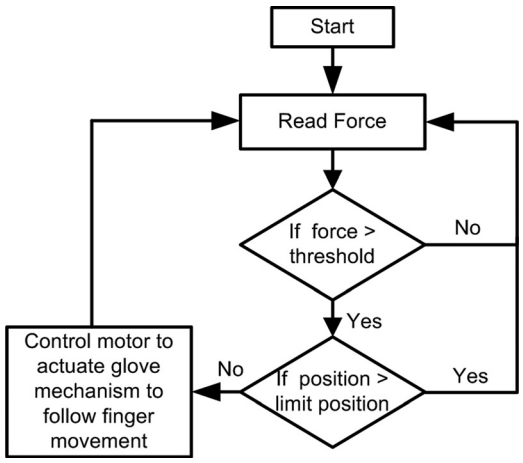

Fig. 8 Flowchart of the control algorithm for free motion test

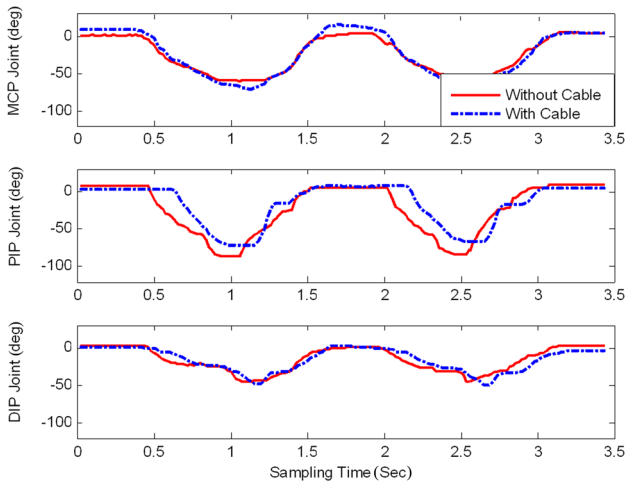

Fig. 9 Human index finger trajectories for two close/open maneuvers acquired by user 1 in test #1

4.2 Measurement of Finger Forces. FSR are used to measure the contact force between the fingertip and the object and the force between the glove and the user's hand. The FSR on the SAFER glove are robust polymer thick film devices that exhibit a decrease in resistance with an increase in force when applied to its surface. They are of high performance and are low in cost. The force sensitivity is optimized for use for human touch control and the actuation force is as low as 0.1 N with a sensitivity range of 10 N.

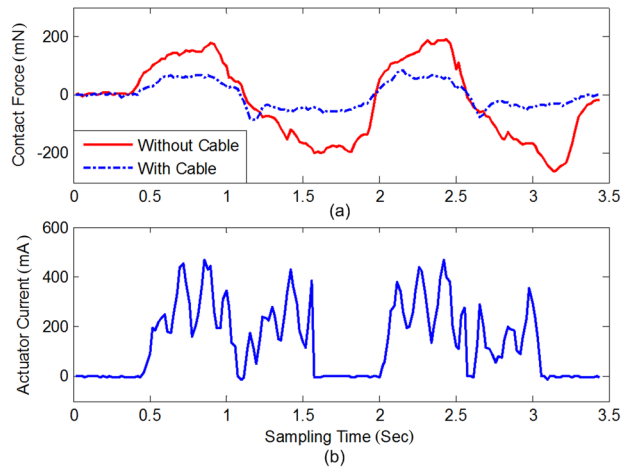

Fig. 10 Contact force (*a*) and actuator current (*b*) measured in free movement test for user 1

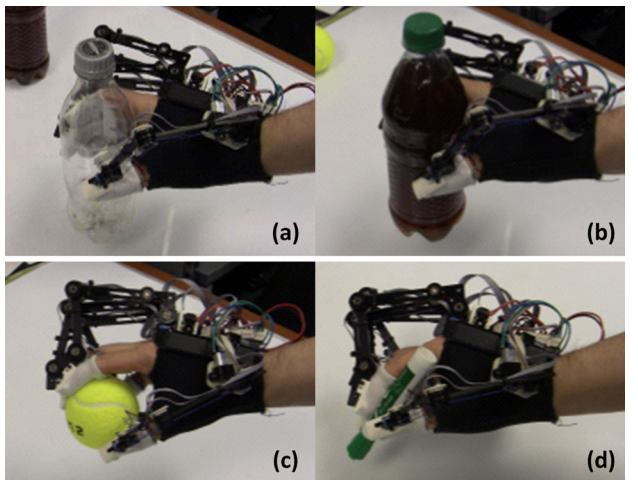

Fig. 11 Demonstration of experiments for grasping different objects with the third generation SAFER glove: (*a*) an empty bottle, (*b*) a bottle of liquid, (*c*) a tennis ball, and (*d*) a marker pen

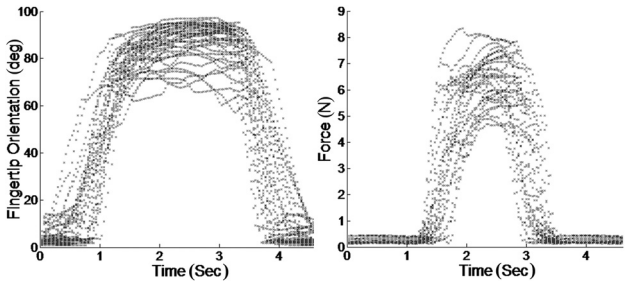

Fig. 12 Demonstration of grasping motion and force reading from the index finger in grasping a bottle of water test: (left) fingertip motion and (right) fingertip force

4.3 Recording Free Motion During Demonstration. The ability to perform free motion is a basic evaluation criterion of haptic devices [32]. The haptic glove's user should be able to move his/her fingers freely without feeling resistance or inertia from the glove during free motion mode (i.e., the state with zero force input). The resistance and inertia should be compensated for via a real-time control algorithm (flowchart shown in Fig. 8) based on the force and position sensors input. It was determined that the force between the glove and the finger should be as small as

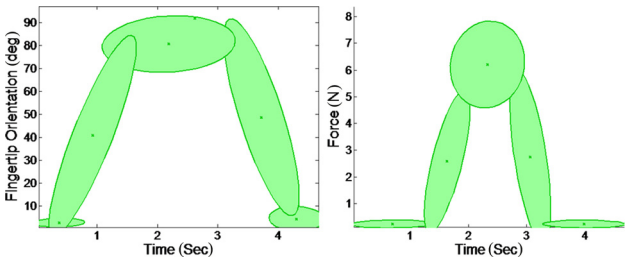

Fig. 13 The GMM model result: (left) finger motion and (right) finger force

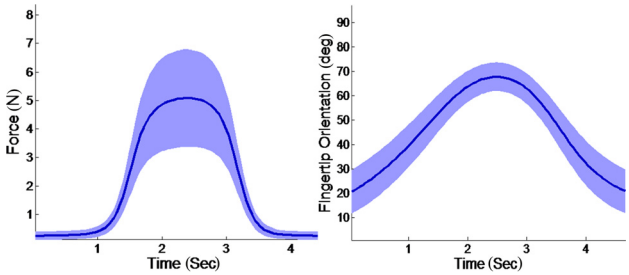

Fig. 14 Generated force trajectory with GMR: (left) finger motion and (right) finger force

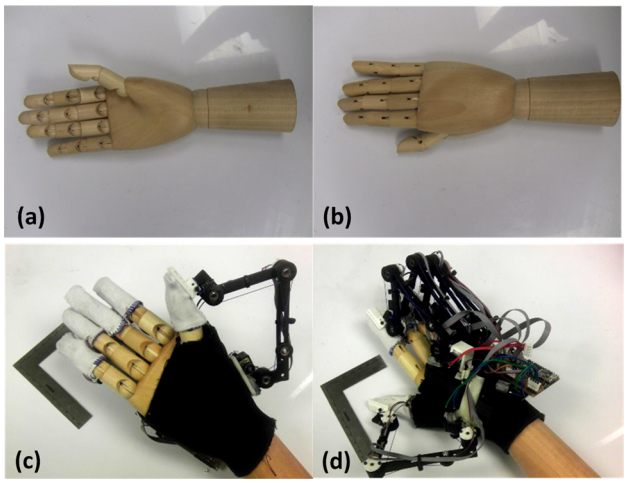

Fig. 15 The glove system (third generation) fitted on a wooden hand: (*a*) and (*b*) the front and back views of the wooden hand and (*c*) and (*d*) the front and back views of the glove system worn on the wooden hand

possible in free motion. If the device is controlled and the force set to zero, the glove will follow the movement of the user's fingers. Thus, the user cannot feel the resistance force.

An experiment that evaluates this free motion was established to demonstrate the effectiveness of friction compensation in the control algorithm. In this experiment, four male and one female subjects were asked to wear the glove prototype and to move all fingers in close/open maneuvers, in two different modes: without cabling and with cabling. In the "without cabling" mode, all the actuation cables were removed. Without the friction, the fingers' mechanisms move easily even under a small external force. The "with cabling" mode is the normal glove mechanism system with the cables installed and force feedback enabled. In this second mode, the control algorithm actively positions the actuators to ensure that the glove mechanism tracks the fingers' movement.

In both modes, each user was asked to repeat two close–open hand maneuvers five times in approximately 3 s. The 15 joint angle sensors of the glove measured the joints angles at a sampling frequency of 300 Hz. Before recording the data, each user spent several minutes to get used to the system.

The graphical results for two close/open maneuvers acquired by the first user's index finger in test no. 1 are reported herein as a representative example of the total test results. Five parameters are displayed for the two modes in Figs. 9 and 10: the three measured joint angle trajectories, the contact force, and the actuator current (note that the actuator current is not applicable to the without cabling mode because the motor is not used). In each test, the user took about 1 s for one full close/open maneuver. At this speed, the maximum contact forces were approximately 200 mN in the without cable mode and 100 mN in the with cable mode. This result shows that the mechanism's internal resistance can be effectively compensated by the control algorithm.

5 Experiments: Sensing the Hand Module

5.1 Demonstration Experiment. The demonstration experiment is performed to record finger movements and force during grip patterns of 12 volunteers between the ages of 20 and 69 yr. The volunteers who participated in this test exhibited normal, pain-free hand function.

The testing tasks involved grasping and lifting an empty bottle, grasping and lifting a bottle full of liquid (500 g), squeezing a tennis ball, and holding a marker pen as if preparing to write (Fig. 11). Participants were then asked to repeat each task three times in about 5–10 s after getting comfortable wearing the SAFER glove. In this test, the glove was controlled to track the finger movement by minimizing the force between the finger and the glove throughout the motion. Figure 12 shows a representative example of the test results of the demonstration for grasping force

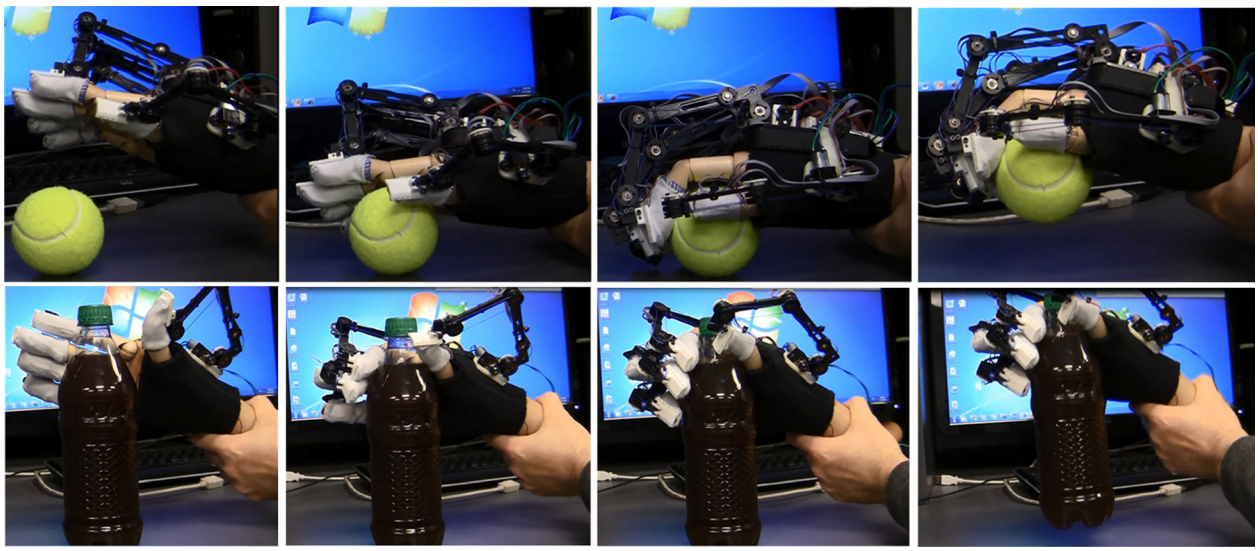

Fig. 16 Wooden hand executing manipulation tasks. Top row: the wooden hand approached the tennis ball (by the author), grasped it, and lifted it (assisted by the author) from the table. Bottom row: the wooden hand was controlled to grasp a bottle of water.

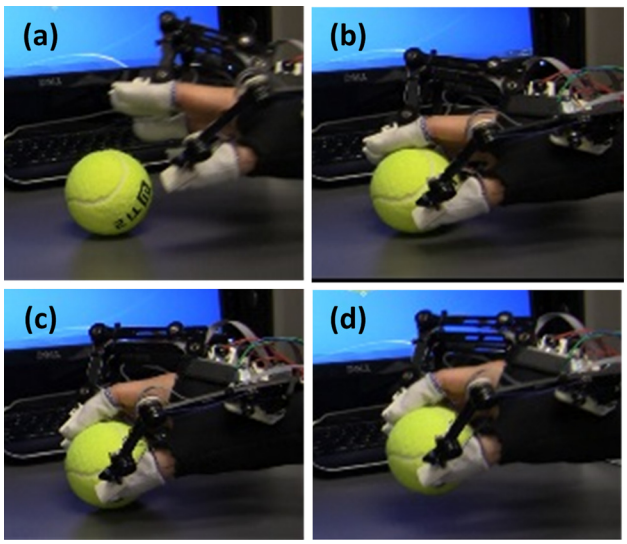

Fig. 17 Assisting hand motion experiment: the user's hand approaches the tennis ball, grasps it with the glove, and lifts it from the table

read from the index finger when grasping a bottle of liquid [27]. The GMM model of the force and motion dataset during 36 trials (12 users, 3 trials per person) of grasping demonstration is shown in Fig. 13. Since the grasping process naturally has three major states, the number of major mixture components is selected to be three. These are listed as: grasp the object, lift and place back the object, and release the object. The other two "minor" Gaussians shown in Fig. 13 relate to the beginning and ending points where the hand is idle. Figure 14 shows the generated GMR trajectories, which work as input signals to the controller module of the SAFER glove [27].

5.2 Passive Hand Actuation Experiment. In this experiment, the SAFER glove is attached to a passive wooden hand (Fig. 15) that does not produce any reactive forces by itself. Figure 16 displays snapshots of the wooden hand executing manipulation tasks. The wooden hand cannot pick up a pen, and the results of the empty bottle are similar to those of the full bottle, so these two experiments are not shown here. Figure 18 shows the actual force trajectories of the glove applied for grasping different objects. In the first stage, the wooden hand is rotated by the glove until the fingers contact the object, and the contact force remains

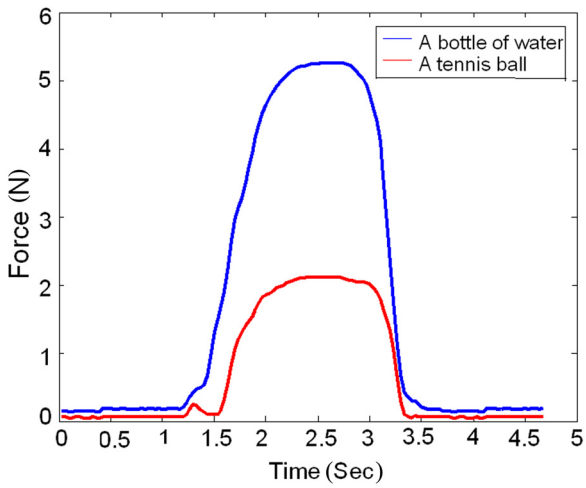

Fig. 18 The force results (index finger) recorded from the glove grasping the objects from Fig. 16

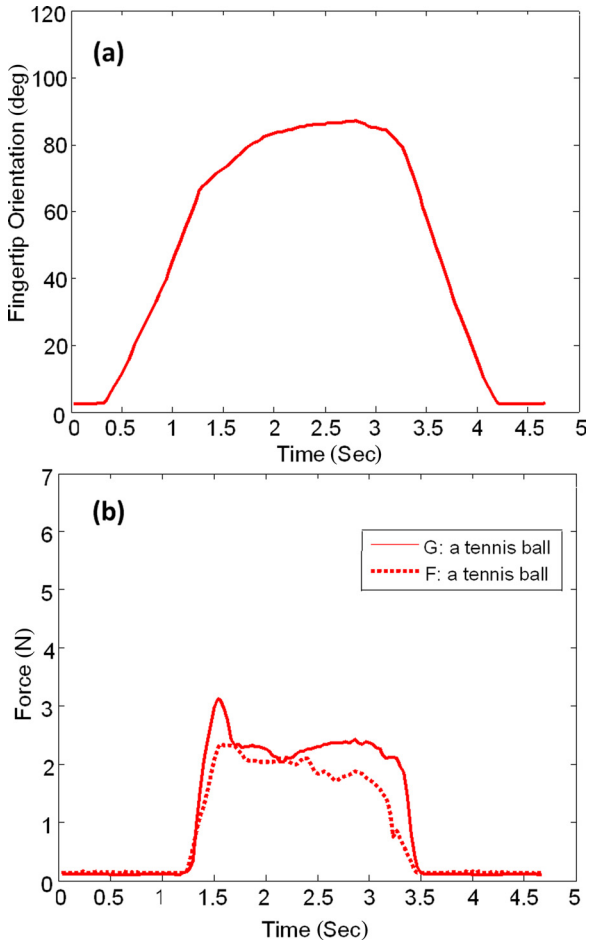

Fig. 19 Index finger motion and force during assisting grasping of a tennis ball: (*a*) fingertip trajectories and (*b*) force between the finger and the glove (G, solid line) and force between the finger and the object (F, dotted line)

at a small value (almost zero). Then, the wooden hand grasps and picks up the object, while the controller generates appropriate contact force. The wooden hand releases the object in the last stage.

5.3 Hand Motion Assistance Experiment. In this experiment, some of the movement patterns shown in Fig. 4 were generated in a playback fashion to assist a "weakened" hand in order to accomplish these movements. Since the subjects had healthy hands, they were asked to passively follow the glove movement without applying any active force. The glove was programed to actively drive the user's fingers to follow the force trajectory from the learned data. Figure 17 shows sample snapshots of assisting hand motion for grasping a tennis ball. The index finger force results during this test are shown in Fig. 18. The other fingers' motions have similar results. Figure 19 displays similar pattern of fingertip trajectories and contact force between the finger and object, which demonstrate that the glove was controlled smoothly and effectively. It can be seen from Fig. 19(*b*) that the force between the finger and the glove that is used to drive the hand motion is larger than the force between the finger and the object. This result demonstrates that the glove is driving the hand as intended. More details on the experiments are available in Ref. [27].

6 Conclusions

This paper presented the design evolution and sample application of the SAFER glove in hand rehabilitation. A new grasping-learning system was proposed that is designed to record kinematic

and force information of normally functioning hands, process this data, and playback these motions to assist grasping movements, such as grasping a bottle of water for users with weak or impaired hands. The fingertip forces, modeled with a GMM-based machine learning approach, are measured by the SAFER glove. The learned force distributions are then used to generate fingertip force trajectories with a GMR approach. A wooden hand was fitted with the SAFER glove to demonstrate its ability to manipulate the hand and to grasp various objects. Instead of defining a grasping force, force trajectories were used to control the SAFER glove and to actuate/assist finger movements. To further demonstrate that the hand can be driven solely by this haptic mechanism, force sensor readings placed between each finger and the mechanism are presented. These experimental results validate the potential of the proposed system in future hand rehabilitation therapy.

Future work will further improve the learning system with additional experiments involving the use of the glove on healthy hands. Future work will include: (1) developing 3D tracking of the hand–glove system; (2) sensing the hand's intention to move as a means to autonomously activate the glove mechanism; and (3) performing "multiple device cooperation" such as synchronizing the motion of left and right SAFER gloves to assist both hands to use a fork and knife at the same time, for example.

Acknowledgment

We would like to acknowledge Mr. Wael Saab for his help with editing the paper.

References

[1] Demain, S., Metcalf, C. D., Merrett, G. V., Zheng, D., and Cunningham, S., 2013, "A Narrative Review on Haptic Devices: Relating the Physiology and Psychophysical Properties of the Hand to Devices for Rehabilitation in Central Nervous System Disorders," Disability Rehabil. Assistive Technol., **8**(3), pp. 181–189.

[2] Heo, P., Gu, G. M., Lee, S., Rhee, K., and Kim, J., 2012, "Current Hand Exoskeleton Technologies for Rehabilitation and Assistive Engineering," Int. J. Precis. Eng. Manuf., **13**(5), pp. 807–824.

[3] Mao, Y., and Agrawal, S. K., 2012, "Design of a Cable-Driven Arm Exoskeleton (CAREX) for Neural Rehabilitation," IEEE Trans. Rob., **28**(4), pp. 922–931.

[4] Sugar, T. G., He, J., Koeneman, E. J., Koeneman, J. B., Herman, R., Huang, H., Schultz, R. S., Herring, D. E., Wanberg, J., Balasubramanian, S., Swenson, P., and Ward, J. A., 2007, "Design and Control of RUPERT: A Device for Robotic Upper Extremity Repetitive Therapy," IEEE Trans. Neural Syst. Rehabil. Eng., **15**(3), pp. 336–346.

[5] Mehrholz, J., and Marcus, P., 2012, "Electromechanical-Assisted Gait Training After Stroke: A Systematic Review Comparing End-Effector and Exoskeleton Devices," J. Rehabil. Med., **44**(3), pp. 193–199.

[6] Yin, Y. H., Fan, Y. J., and Xu, L. D., 2012, "EMG and EPP-Integrated Human–Machine Interface Between the Paralyzed and Rehabilitation Exoskeleton," IEEE Trans. Inf. Technol. Biomed., **16**(4), pp. 542–549.

[7] Tubiana, R., Thomine, J., and Mackin, E., 1984, *Examination of the Hand and Upper Limb*, WB Saunders, Philadelphia, PA, p. 79.

[8] Lee, S. W., Landers, K. A., and Hyung-Soon, P., 2014, "Development of a Biomimetic Hand Exotendon Device (BiomHED) for Restoration of Functional Hand Movement Post-Stroke," IEEE Trans. Neural Syst. Rehabil. Eng., **22**(4), pp. 886–898.

[9] Jack, D., Boian, R., Merians, A., Adamovich, S., Tremaine, M., Recce, M., Burdea, G., and Poizner, H., 2000, "A Virtual Reality-Based Exercise Program for Stroke Rehabilitation," 4th ACM SIGCAPH Conference on Assistive Technologies (Assets '00), Arlington, VA, Nov. 13–15, pp. 56–63.

[10] Heuser, A., Kourtev, H., Winter, S., Fensterheim, D., Burdea, G., Hentz, V., and Forducey, P., 2007, "Telerehabilitation Using the Rutgers Master II Glove Following Carpal Tunnel Release Surgery: Proof-of-Concept," IEEE Trans. Neural Syst. Rehabil. Eng., **15**(1), pp. 43–49.

[11] VRLogic, 1999, "Datagloves—Cyberglove," VRLogic GmbH, Dieburg, Germany, http://www.vrlogic.com/index.php/en/datagloves/cyberglovesystems

[12] Connelly, L., Jia, Y., Toro, M. L., Stoykov, M. E., Kenyon, R. V., and Kamper, D. G., 2010, "A Pneumatic Glove and Immersive Virtual Reality Environment for Hand Rehabilitative Training After Stroke," IEEE Trans. Neural Syst. Rehabil. Eng., **18**(5), pp. 551–559.

[13] Arata, J., Ohmoto, K., Gassert, R., Lambercy, O., Fujimoto, H., and Wada, I., 2013, "A New Hand Exoskeleton Device for Rehabilitation Using a Three-Layered Sliding Spring Mechanism," IEEE International Conference on Robotics and Automation (ICRA), Karlsruhe, Germany, May 6–10, pp. 3902–3907.

[14] Diftler, M. A., Ihrke, C. A., Bridgwater, L. B., Davis, D. R., Linn, D. M., Laske, E. A., Ensley, K. G., and Lee, J. H., 2014, "RoboGlove—A Robonaut Derived Multipurpose Assistive Device," International Conference on Robotics and Automation (ICRA), Hong Kong, May 31–June 7.

[15] Ma, Z., and Ben-Tzvi, P., 2015, "RML Glove—An Exoskeleton Glove Mechanism With Haptics Feedback," IEEE/ASME Trans. Mechatronics, **20**(2), pp. 641–652.

[16] Kawasaki, H., Ito, S., Ishigure, Y., Nishimoto, Y., Aoki, T., Mouri, T., Sakaeda, H., and Abe, M., 2007, "Development of a Hand Motion Assist Robot for Rehabilitation Therapy by Patient Self-Motion Control," IEEE International Conference on Robotic Rehabilitation (ICORR 2007), Noordwijk, The Netherlands, June 13–15, pp. 234–240.

[17] Dovat, L., Lambercy, O., Gassert, R., Maeder, T., Milner, T., Leong, T. C., and Burdet, E., 2008, "HandCARE: A Cable-Actuated Rehabilitation System to Train Hand Function After Stroke," IEEE Trans. Neural Syst. Rehabil. Eng., **16**(6), pp. 582–591.

[18] Endo, T., Tanimura, S., and Kawasaki, H., 2013, "Development of Tool-Type Devices for a Multi-Fingered Haptic Interface Robot," IEEE Trans. Rob., **29**(1), pp. 68–81.

[19] QAL Medical, 2014, "6000X WaveFlex Hand CPM," QAL Medical LLC, Marinette, WI, http://qalmedical.com/waveflex-hand-cpm-device/

[20] Schabowsky, C., Godfrey, S., Holley, R., and Lum, P., 2010, "Development and Pilot Testing of HEXORR: Hand EXOskeleton Rehabilitation Robot," J. NeuroEng. Rehabil., **7**(1), p. 36.

[21] Takahashi, C. D., Der-Yeghiaian, L., Le, V., and Cramer, S., 2005, "A Robotic Device for Hand Motor Therapy After Stroke," IEEE 9th International Conference on Rehabilitation Robotics: Frontiers of the Human-Machine Interface (ICORR 2005), Chicago, IL, June 28–July 1, pp. 17–20.

[22] Kadowaki, Y., Noritsugu, T., Takaiwa, M., Sasaki, D., and Kato, M., 2011, "Development of Soft Power-Assist Glove and Control Based on Human Intent," J. Rob. Mechatronics, **23**(2), pp. 281–291.

[23] Polygerinos, P., Wang, Z., Galloway, K. C., Wood, R. J., and Walsh, C. J., 2014, "Soft Robotic Glove for Combined Assistance and At-Home Rehabilitation," Rob. Auton. Syst., **73**, pp. 135–143.

[24] Vanoglio, F., Luisa, A., Garofali, F., and Mora, C., 2013, "Evaluation of the Effectiveness of Gloreha (Hand Rehabilitation Glove) on Hemiplegic Patients. Pilot Study," XIII Congress of Italian Society of Neurorehabilitation, Bari, Italy, Apr. 18–20.

[25] Ma, Z., and Ben-Tzvi, P., 2015, "Sensing and Force-Feedback Exoskeleton (SAFE) Robotic Glove," IEEE Trans. Neural Syst. Rehabil. Eng., **23**(6), pp. 992–1002.

[26] Ma, Z., and Ben-Tzvi, P., 2015, "Design and Optimization of a Five-Finger Haptic Glove Mechanism," ASME J. Mech. Rob., **7**(4), p. 041008.

[27] Ma, Z., Ben-Tzvi, P., and Danoff, J., 2015, "Hand Rehabilitation Learning System With an Exoskeleton Robotic Glove," IEEE Trans. Neural Syst. Rehabil. Eng. (in press).

[28] Marin, J.-M., Mengersen, K., and Robert, C. P., 2005, "Bayesian Modelling and Inference on Mixtures of Distributions," *Handbook of Statistics 25*, Elsevier, Amsterdam, pp. 459–507.

[29] Tomasi, G., van den Berg, F., and Anderson, C. A., 2004, "Correlation Optimized Warping and Dynamic Time Warping as Preprocessing Methods for Chromatographic Data," J. Chemom., **18**(5), pp. 231–241.

[30] Ren, Y., Park, H. S., and Zhang, L. Q., 2009, "Developing a Whole-Arm Exoskeleton Robot With Hand Opening and Closing Mechanism for Upper Limb Stroke Rehabilitation," IEEE International Conference on Rehabilitation Robotics (ICORR 2009), Kyoto, Japan, June 23–26, pp. 761–765.

[31] Burdea, G., and Coiffet, P., 2003, *Virtual Reality Technology*, 2nd ed., Wiley, New York.

[32] Ohashi, T., Szemes, P., Korondi, P., and Hashimoto, H., 1999, "Nonlinear Disturbance Compensation for Haptic Device," IEEE International Symposium on Industrial Electronics (ISIE '99), Bled, Slovenia, July 12–16, pp. 304–309.